Supporting Information

Molecular Dynamic Simulations of Liquid Structure and Fast Growth of $Y_3Al_5O_{12}$

Xianjie Zhang[a,#],Feng Liu [b,#], Kunfeng Chen[c], Guiling Zhuang[a], Chao Peng[b], Dongfeng Xue[b,*]

a. Institute of Industrial Catalysis, State Key Laboratory Breeding Base of GreenChemical Synthesis Technology, College of Chemical Engineering, Zhejiang University of Technology, Hangzhou 310032, P.R. China.

b. Multiscale Crystal Materials Research Center, Shenzhen Institute of Advanced Technology, Chinese Academy of Sciences, Shenzhen 518055, China;.

c. State Key Laboratory of Crystal Materials, Institute of Novel Semiconductors, Shandong University, Jinan 250100, China.

Table S1 Calculation of YAG Structure and Properties Using Potential Parameters (Compared with Experimental Structural/Property Information)

	Simulations				
	This work	Du's work[1]	Schuh[2]	DFT-LDA[3]	Experimental
a(Å)	12.021	12.024	12.026	11.904	12.006[4]
Al-O distance (Å)	1.768/1.927	1.751/1.948	1.779/1.917	1.743/1.917	1.754/1.938[4]
Y-O distance (Å)	2.310/2.448	2.320/2.440	2.271/2.472	2.280/2.407	2.317/2.437[4]
Bulk modulus (GPa)	192.6	189.4	218	220.7	189[5],185[6]
Shear modulus (GPa)	102.5	101.8	120	—	
Young's modulus (GPa)	242.1	240.0	314	—	
C_{11} (GPa)	317.2	313.6	395	—	339[5]
C_{22} (GPa)	108.3	108.0	135	—	114[5]
C_{33} (GPa)	130.0	127.4	117	—	116[5]

RDF calculated by the AIMD[7] and classic MD method (FF) show in the Figure S1(a). The positions of the peaks are consistent. The relative proportion among the various coordination unit (AlOx (x=3, 4, 5, 6), YOx (x=4, 5, 6, 7, 8, 9)) and the angles distribution for O-Al-O and O-Y-O is consistent with that in the AIMD, as shown in the Figure 1S(b) and (c). We have also tested some properties of the crystal, as shown in the Table S1, such as lattice constant, elastic constant, angle, etc., and the results are very close to the values from the experiment. So, this classic potential is suitable to describe the YAG melt and crystal.

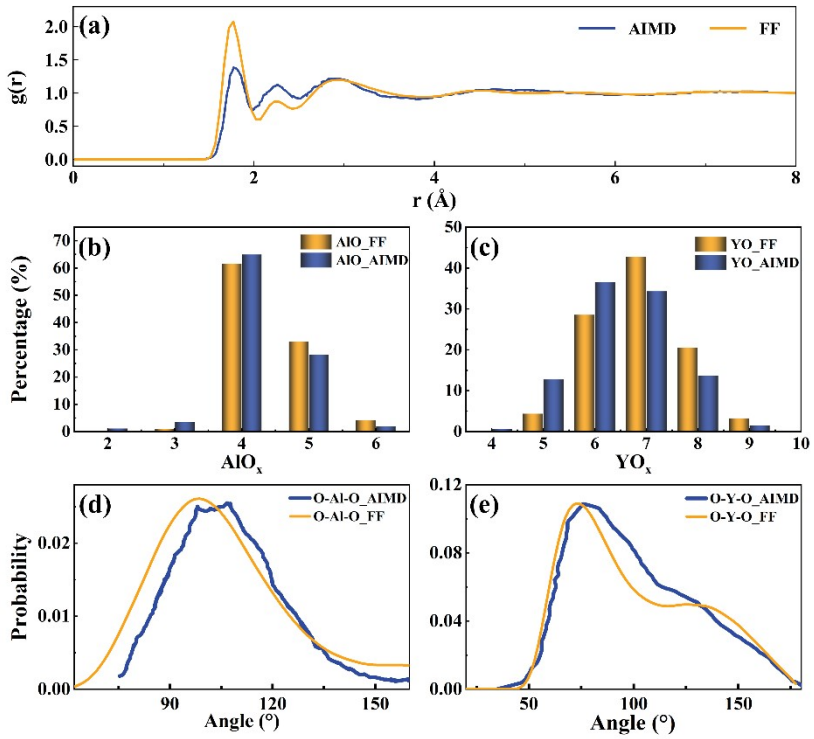

Figure S1 RDF, relative proportion among the various coordination unit (AlOx (X=3,45, 6), YOx (x=4, 5, 6, 7, 8, 9)) and BAD for O-Al-O and O-Y-O calculated by theAIMD[7] and classic MD method (FF).

The melting point of YAG was calculated by the solid-liquid coexistence method introduced by Morris and coworkers,[8, 9] which has been used in metal systems widely. Firstly, the lattice parameters of the bulk YAG crystal as a function of temperature at 1 bar were determined by running the NPT ensemble. To obtain the solid-liquid coexistence structure of the YAG, a simulation box consisting of periodic solid units was structured, where the z-direction was normal to the solid-liquid interface and was longer than the other two directions. Then, the ions in the central half of the simulation box (grouped *A*) are fixed while the other ions in simulation box can be relaxed by performing the NP_zT ensemble at the temperature of 1000 K above the melting point. The length of the simulation box in the direction parallel to the solid-liquid interface were fixed at running the NP_zT ensemble, allowing the length of the simulation box to evolve dynamically in the normal direction with zero imposed stress. Subsequently, the refined melting point of the YAG was derived by performing NPH ensemble (constant atom number, pressure, and enthalpy) and the length of the simulation box parallel to the interface was adjusted according to the temperature-lattice constant functions. The whole process was repeated until the stress between the solid-liquid interface was zero. Ultimately, the melting point of YAG calculated was 2100 K when the solid-liquid interface was stable, which was agree with the experimental value approximately.

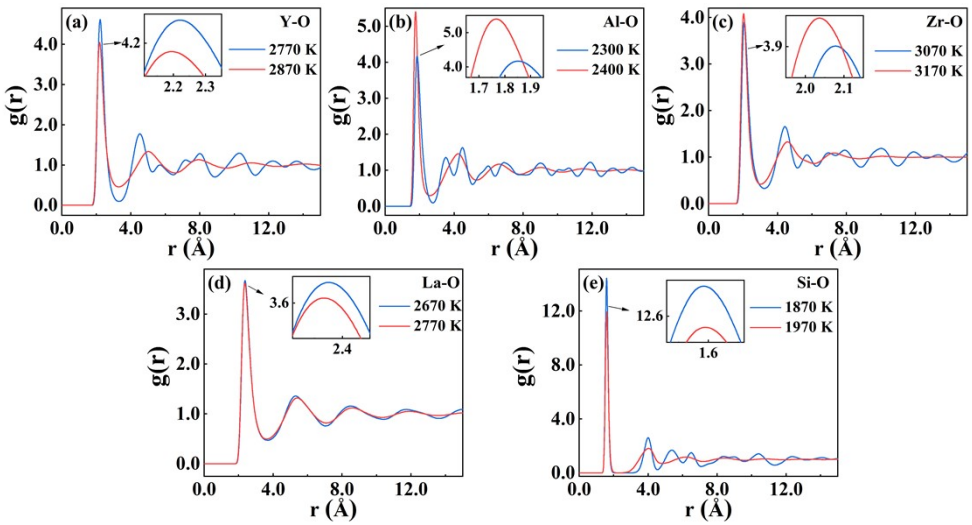

Figure S2 Radial distribution functions of the five oxide systems: (a) Y_2O_3, (b) Al_2O_3, (c) ZrO_2, (d) La_2O_3 and (e) SiO_2

Table S2 The bond length and coordination number for the five oxide systems.

Composition	Crystal	Solid		Liquid		
	mean coord	Temp	first peak	Temp	mean coord	first peak
A-O	A-O	(K)	A-O(Å)	(K)	A-O	A-O(Å)
Y_2O_3	6	2770	2.22	2870	5.5[10]	2.20
Al_2O_3	5,6	2300	1.85	2400	4.5[10]	1.77
ZrO_2	7,8	3070	2.08	3170	6.1[10]	2.04
La_2O_3	7	2670	2.38	2770	5.9[10]	2.37
SiO_2	4	1870	1.59	1970	4.0[10]	1.59

Table S3 The ratio of sharing types of cationic polyhedra

Cationic polyhedra	Temperature (K)	Sharing (%)			
		Isolated	Corner	Edge	Face
$[YO_x]$- $[YO_x]$	300 (crystal)	0.0%	50.0%	50.0%	0.0%
(Y_2O_3)	2770(solid)	0.0%	51.6%	48.0%	0.5%
	2870 (liquid)	0.0%	56.4%	34.4%	9.2%
$[AlO_x]$- $[AlO_x]$	300 (crystal)	0.0%	69.2%	23.1%	7.7%
(Al_2O_3)	2300(solid)	0.0%	68.8%	23.6%	7.6%

	2400 (liquid)	0.0%	81.0%	18.2%	0.8%
$[ZrO_x]$- $[ZrO_x]$	300 (crystal)	0.0%	0.0%	100.0%	0.0%
(ZrO_2)	3070(solid)	0.0%	25.9%	65.3%	8.8%
	3170 (liquid)	0.0%	58.8%	34.3%	7.0%
$[LaO_x]$- $[LaO_x]$	300 (crystal)	0.0%	20.0%	80.0%	0.0%
(La_2O_3)	2670(solid)	0.0%	45.2%	36.9%	17.9%
	2770 (liquid)	0.0%	51.0%	34.7%	14.3%
$[SiO_x]$- $[SiO_x]$	300 (crystal)	0.0%	100.0%	0.0%	0.0%
(SiO_2)	1870(solid)	0.0%	100.0%	0.0%	0.0%
	1970 (liquid)	0.0%	99.8%	0.2%	0.0%

The potential model and method used to calculate the RDF, coordination number and oxygen ions number of sharing, for these five systems are the same as those used by Skinner, and the specific calculation details are the same as those used in the YAG systems.

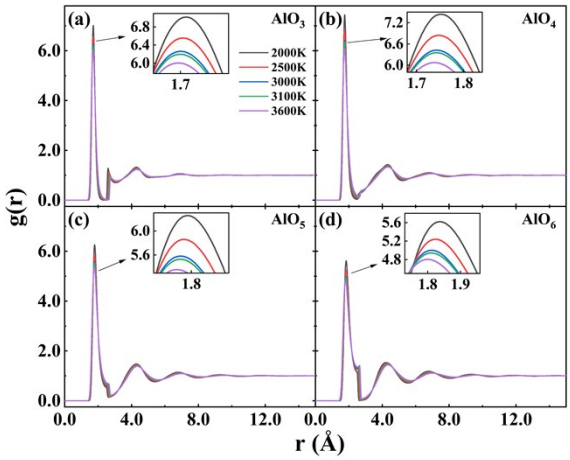

Figure S3 Radial distribution functions calculated base on different $[AlO_x]$ coordination units: (a) $[AlO_3]$, (b) $[AlO_4]$, (c) $[AlO_5]$ and (d) $[AlO_6]$. For example, in the subgraph (a), only take the Al^{3+} with three oxygen coordination number into consideration.

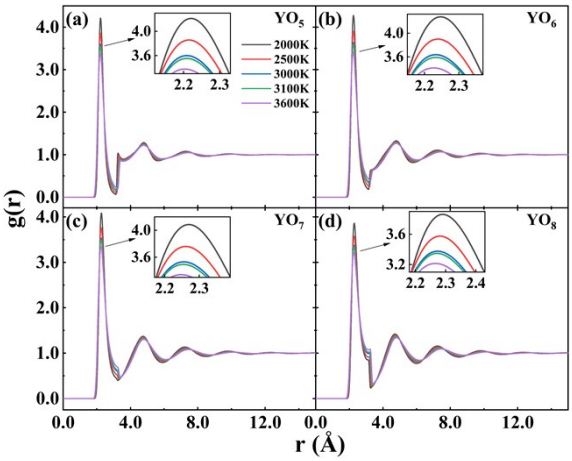

Figure S4 Radial distribution functions calculated base on different $[YO_x]$ coordination units: (a) $[YO_5]$, (b) $[YO_6]$, (c) $[YO_7]$ and (d) $[YO_8]$.

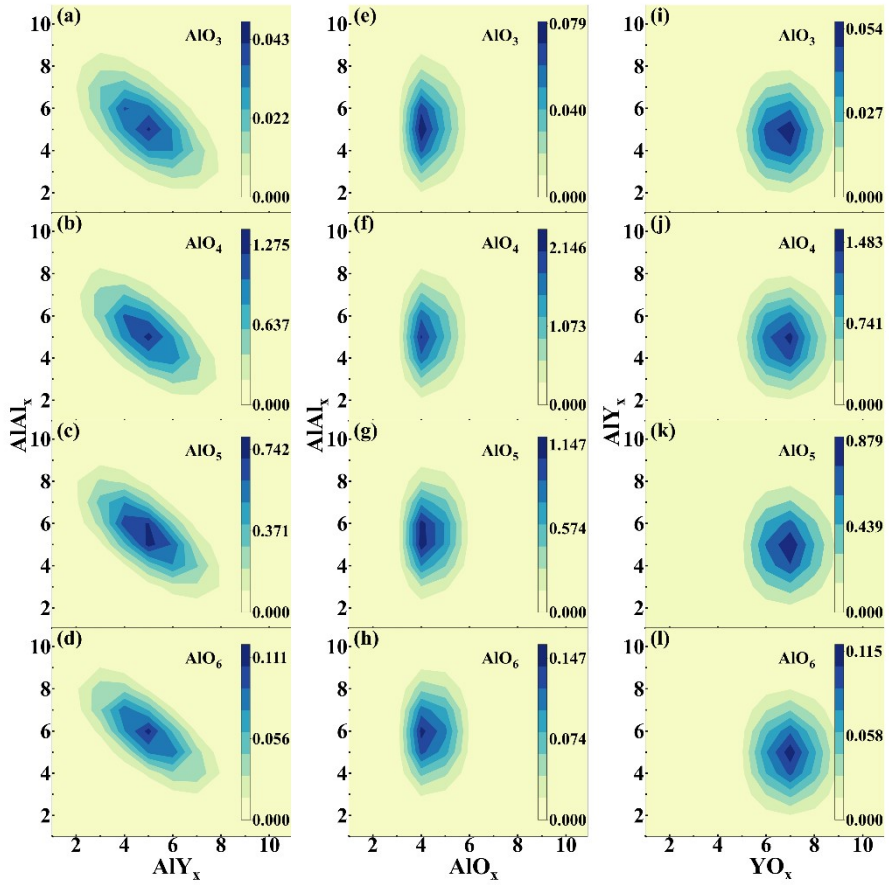

Figure S5 Local structure around the various [AlO_x] in the melt at 2500 K. Here, the local structure described by the number of nearest neighbor ions around central ions. Firstly, AlY_x represent the number of nearest neighbors Y^{3+} around the central Al^{3+}, and x is the number of Y^{3+}. Furthermore, $AlAl_x$ and AlY_x also can be understood by this definition. Note, AlO_x and YO_x represent the oxygen coordination number for the cation (Al^{3+} and Y^{3+} respectively) belong to the nearest neighbors of central Al^{3+}. (a-d): the occurrence frequency for different local structure (described by the AlY_x and $AlAl_x$) around central Al^{3+} in various [AlO_x] coordination unit. (e-h): the occurrence frequency for different local structure described by the AlO_x and $AlAl_x$. (i-l): the occurrence frequency for different local structure described by YO_x and AlY_x..

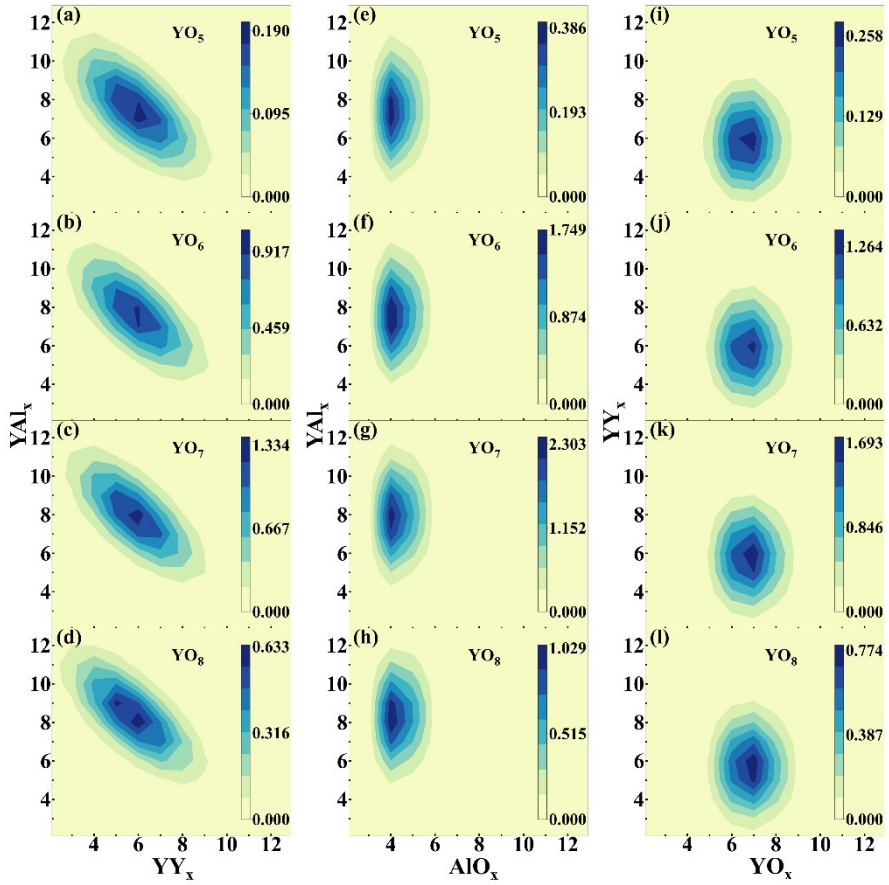

Figure S6 Local structure of Y^{3+} in the melt at 2500 K. Here, the local structure also described by the number of nearest neighbor ions around central ions. Firstly, YAl_x represent the number of nearest neighbors Al^{3+} around the central Y^{3+}, and x is the number of Al^{3+}. Furthermore, YY_x, YAl_x also can be understood by this definition. Note, AlO_x and YO_x represent the oxygen coordination number for the cation (Al^{3+} and Y^{3+} respectively) belong to the nearest neighbors of central Y^{3+}. (a-d): the relative percentage for different local structure (described by the YAl_x and YY_x) of central Y^{3+} in various [YO_x] coordination unit, (e-h): the relative percentage for different local structure described by the AlO_x and YAl_x, (i-l): the relative percentage for different local structure described by the YO_x and YY_x.

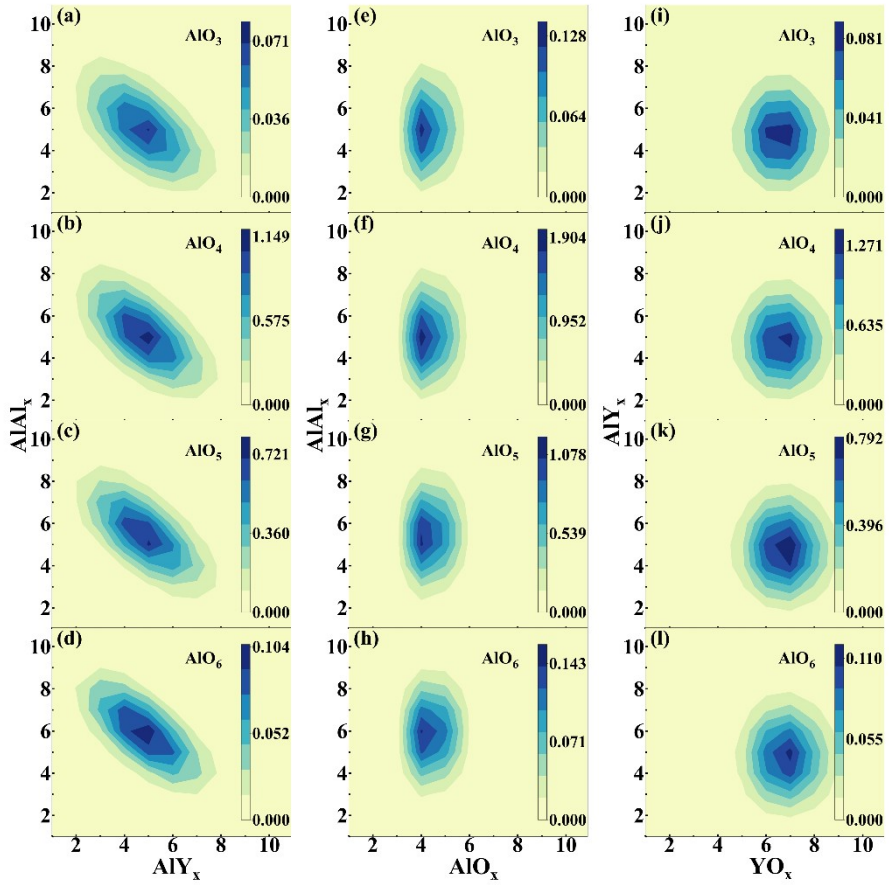

Figure S7 Local structure around the various [AlO_x] in the melt at 3000 K. (a-d): the occurrence frequency for different local structure (described by the AlY_x and $AlAl_x$) around central Al^{3+} in various [AlO_x] coordination unit. (e-h): the occurrence frequency for different local structure described by the AlO_x and $AlAl_x$. (i-l): the occurrence frequency for different local structure described by YO_x and AlY_x.

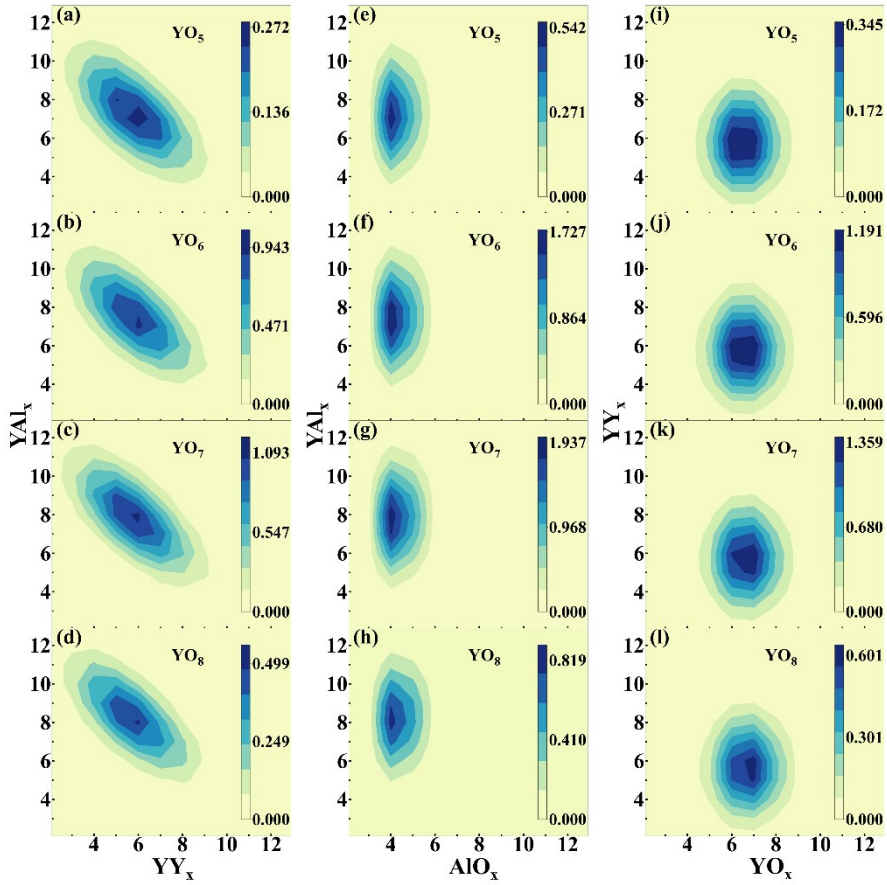

Figure S8 Local structure of Y^{3+} in the melt at 3000 K. Here, the local structure also described by the number of nearest neighbor ions around central ions. (a-d): the relative percentage for different local structure (described by the YAl_x and YY_x) of central Y^{3+} in various [YO_x] coordination unit, (e-h): the relative percentage for different local structure described by the AlO_x and YAl_x, (i-l): the relative percentage for different local structure described by the YO_x and YY_x..

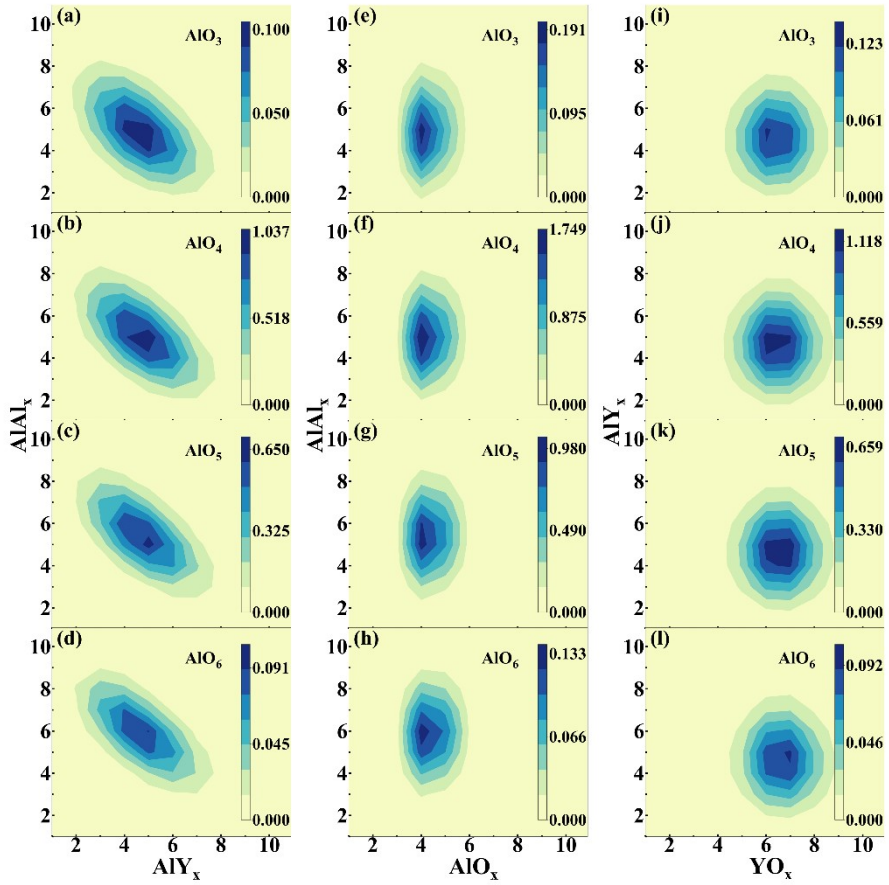

Figure S9 Local structure around the various [AlO_x] in the melt at 3500 K. Here, the local structure described by the number of nearest neighbor ions around central ions. (a-d): the occurrence frequency for different local structure (described by the AlY_x and $AlAl_x$) around central Al^{3+} in various [AlO_x] coordination unit. (e-h): the occurrence frequency for different local structure described by the AlO_x and $AlAl_x$. (i-l): the occurrence frequency for different local structure described by YO_x and AlY_x.

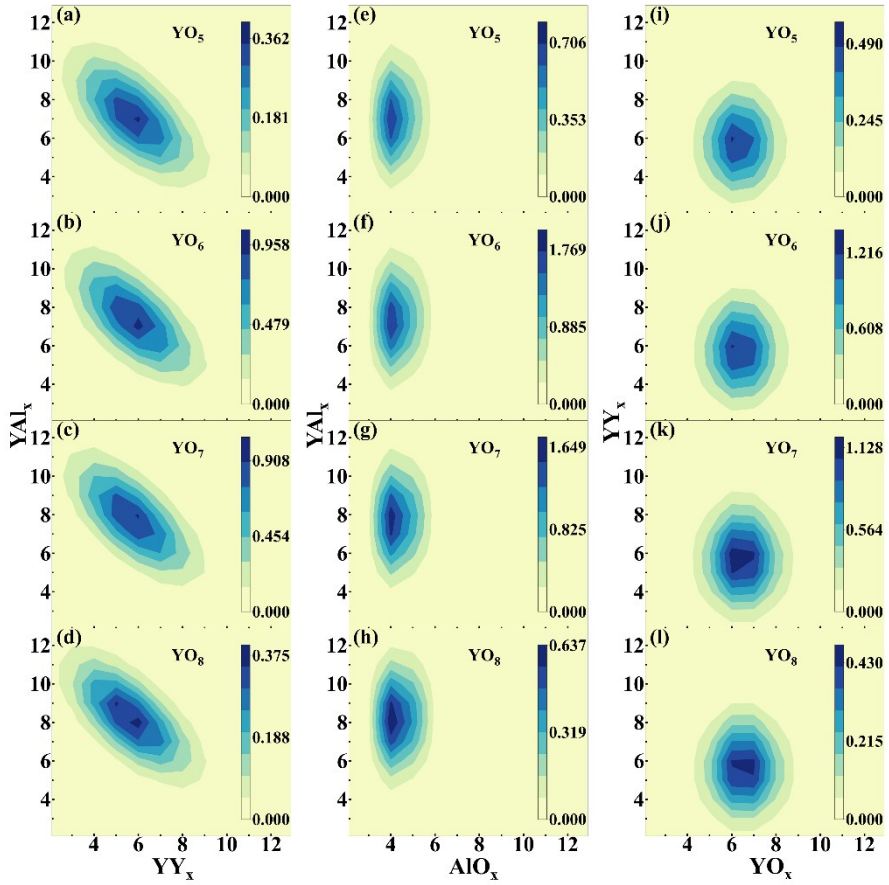

Figure S10 Local structure of Y^{3+} in the melt at 3500 K. Here, the local structure also described by the number of nearest neighbor ions around central ions. (a-d): the relative percentage for different local structure (described by the YAl_x and YY_x) of central Y^{3+} in various [YO_x] coordination unit, (e-h): the relative percentage for different local structure described by the AlO_x and YAl_x, (i-l): the relative percentage for different local structure described by the YO_x and YY_x.

Reference

1. Du, J., Molecular dynamics simulations of the structure and properties of low silica yttrium aluminosilicate glasses. *Journal of the American Ceramic Society* **2009,** *92* (1), 87-95.
2. Schuh, L.; Metselaar, R.; Catlow, C., Computer modelling studies of defect structures and migration mechanisms in yttrium aluminium garnet. *Journal of the European Ceramic Society* **1991,** *7* (2), 67-74.
3. Xu, Y.-N.; Ching, W., Electronic structure of yttrium aluminum garnet (Y 3 Al 5 O 12). *Physical Review B* **1999,** *59* (16), 10530.
4. Nakatsuka, A.; Yoshiasa, A.; Yamanaka, T., Cation distribution and crystal chemistry of Y3Al5− xGaxO12 (0≤ x≤ 5) garnet solid solutions. *Acta Crystallographica Section B: Structural Science* **1999,** *55* (3), 266-272.
5. Stoddart, P.; Ngoepe, P.; Mjwara, P.; Comins, J.; Saunders, G., High‐temperature elastic constants of yttrium aluminum garnet. *Journal of applied physics* **1993,** *73* (11), 7298-7301.
6. Clark, A.; Strakna, R., Elastic constants of single‐crystal YIG. *Journal of Applied Physics* **1961,** *32* (6), 1172-1173.
7. Cristiglio, V.; Hennet, L.; Cuello, G. J.; Johnson, M. R.; Fernandez-Martinez, A.; Fischer, H. E.; Pozdnyakova, I.; Zanghi, D.; Brassamin, S.; Brun, J. F.; Price, D. L., Ab-initio molecular dynamics simulations of the structure of liquid aluminates. *J. Non-Cryst. Solids* **2007,** *353* (18-21), 1789-1792.
8. Morris, J. R.; Wang, C.; Ho, K.; Chan, C. T., Melting line of aluminum from simulations of coexisting phases. *Physical Review B* **1994,** *49* (5), 3109.
9. Morris, J. R.; Song, X., The melting lines of model systems calculated from coexistence simulations. *The Journal of chemical physics* **2002,** *116* (21), 9352-9358.
10. Parise, J.; Benmore, C.; Weber, J.; Du, J.; Neuefeind, J.; Tumber, S., Low Cation Coordination in Oxide Melts. *Physical Review Letters* **2014,** *112* (BNL-108193-2015-JA).